Article

Journal of
Nanoscience and Nanotechnology
Vol. 15, 2032–2039, 2015
www.aspbs.com/jnn

Copyright © 2015 American Scientific Publishers
All rights reserved
Printed in the United States of America

Controllable and Reversible Dispersiblity of Graphene Materials by a Generic Organometallic Functionalization

Weibo Yan, Yanfei Xu, Lu Huang, and Yongsheng Chen*

Key Laboratory of Functional Polymer Materials and Center for Nanoscale Science and Technology, College of Chemistry, Institute of Polymer Chemistry, Nankai University, Tianjin 300071, China

A general and reversible functionalization method has been developed for reduced graphene oxide (rGO) based on a simple reaction sequence. In this sequence, the chemical functionalization of reduced graphene oxide (rGO) was first carried out by a nucleophilic addition of *n*-butyllithium (*n*-BuLi) to rGO sheets, followed by a subsequent coupling step of intermediates $(n\text{-Bu-rGO})^{n-}\text{Li}^{n+}$ with alkyl halide, leading to functionalized rGO with controllable and reversible dispersiblity in either nonpolar or polar solvents depending on the functional groups. Next, the functional groups could be reversibly removed by solvothermal treatment to generate reduced graphene sheets. Then the reduced materials could be again functionalized using the same reaction sequence above with either the same or different functional groups to almost the same extent of the first functionalization cycle.

Keywords: Reduced Graphene Oxide, Controllable, Reversible, Functionalization.

Delivered by Publishing Technology to: Ryan Yan, School of Chemical Studies, NTU
IP: 155.69.4.4 On: Wed, 25 Mar 2015 07:07:32
Copyright: American Scientific Publishers

1. INTRODUCTION

Graphene, with an atomically thin, 2-dimensional structure that consists of sp^2-hybridized carbons, has attracted enormous interest in the area of solid state electronics[1–4] and composite materials[5–13] due to its fascinating electronic and mechanical properties. To implement many of its applications, such as graphene-based organic and polymer composite materials or organic photoelectric devices,[14] and graphene-based chemistry reactions in various media,[15] new strategies to produce dispersions of graphene sheets with good solution processibility in both nonpolar or polar solvents are required.[16–19] The chemical covalent functionalization has been confirmed as an efficient method to increase or improve their solution processibility of fullerenes, carbon nanotubes, and grapheme.[20–23] Covalent addition reactions to the sp^2-hybridized graphene framework are always accompanied by the generation of sp^3-hybridized atoms and, as a consequence, opening a gap in its band structure, which is critical to fulfill potential application in electronics.[24,25] But this might also be considered as a drawback because the outstanding electronic properties of graphene are required in many regards, such as using as transparent electrode film.[24,26–30] So, it is highly demanded that once the attached addends have completed their assignment for solution processing purpose in a given process chain, they could be removed retroactively so that the intrinsic structure of graphene sheets can be recovered. Based on these, development of retro-functionalization of graphene is much required for many applications of graphene-based materials.

It has been reported that C_{60} and carbon nanotube can react with alkyl lithium (RLi), giving alkylated metal fullerides such as $RC_{60}^{-}Li^{+}$ or $(RnMWNT^{n-})Li^{n+}$.[31–33] Recently, it has also been reported that graphite fluoride can react with alkyl lithium reagents to form soluble graphene layers[34] and oxygen-containing groups of GO can efficiently react with the Grignard reagent.[35] While for the graphene material reduced from GO, the functional groups, mainly epoxide and hydroxyl groups, are almost completely removed, and the sp^2-hybridized framework is greatly recovered. So the left active C═C double bonds could be the mainly reactive sites, which could be attacked by many nucleophiles such as lithium alkyls.[19,36–38]

In this work, we report a simple method for retro-functionalization of chemical reduced GO (rGO), which uses *n*-butyllium (*n*-BuLi) to attack the rGO sheets, following by a coupling reaction with different alkyl halides.

*Author to whom correspondence should be addressed.

 1533-4880/2015/15/2032/008 doi:10.1166/jnn.2015.9155

The dispersibility in nonpolar and polar solvents of these functionalized graphene materials can be controlled by attaching different hydrophilic and hydrophobic groups. More importantly, these groups can be partly removed by a simple solvothermal reduction to get the reduced graphene materials, which can be repeatedly functionalized using the same sequence reactions above to restore mostly the solubility of the graphene materials. The structure integrity and conductivity of the graphene materials at each step were thoroughly studied to show the controllability and reversibility of this functionalization strategy.

2. EXPERIMENTAL DETAILS

2.1. Materials

Graphite was obtained from Qingdao Huarun Graphite Co. All alkyl bromide and *n*-butyllium (2.5 mol L^{-1} in *n*-hexane) were obtained from Alfa Aesar. GO was prepared using a modified Hummers method and rGO was prepared by reducing GO according to the literature.[39] All manipulations were carried out under a dry argon atmosphere using standard Schlenk techniques, and solvents were purified by standard procedures.

2.2. Preparation of Functionalizated rGO

Functionalization of rGO: First, rGO (20 mg) was dispersed in dry THF by sonication for 0.5 hour and then reacted with an excess of *n*-BuLi (25 mmol) under argon at − 10 °C for 1 hour. The mixture was then warmed to room temperature and stirred for 48 hours. Then alkyl bromide (25 mmol) (12.5 mmol for carboxymethyl bromide) was added, and the reaction mixture was stirred under argon at room temperature for 48 hours. At last, H_2O (0.5 mL) were slowly added to quench the reaction. Afterwards, the mixture was centrifuged, washed with C_2H_5OH, H_2O and C_2H_5OH successively and then dried under vacuum to obtain the solid product, **R-Bu-rGO-1**: ***i*-octyl-Bu-rGO-1, carboxymethyl-Bu-rGO-1**.

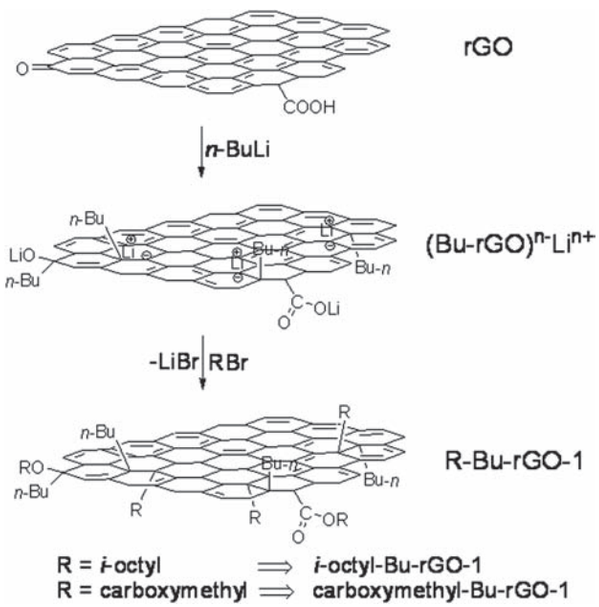

Figure 1. Proposed reactions during the treatment of rGO with *n*-BuLi and then with alkyl bromide, resulting in the alkyl-functionalized-rGO material (R-Bu-rGO-1: *i*-octyl-Bu-rGO-1, carboxymethyl-Bu-rGO-1).

2.3. Solvothermal Reduction of R-Bu-rGO-1

Solvothermal reduction of functionalized rGO: First, functionalized rGO (20 mg) was dispersed in ODCB or NMP by sonication for 0.5 hour. After replacing the air of reaction system with Ar, the mixture was warmed to reflux for 24 hour under slow Ar gas flow. Afterwards, the mixture was centrifuged and then dried under vacuum to obtain the solid product, **R-Bu-rGO-R**:***i*-octyl-Bu-rGO-R, carboxymethyl-Bu-rGO-R**.

2.4. Functionalization of *i*-Octyl-Bu-rGO-R and Carboxymethyl-Bu-rGO-R

The procedure for functionalization of ***i*-octyl-Bu-rGO-R** and **carboxymethyl-Bu-rGO-R** is same as preparation of**R-Bu-rGO-1**. At last we obtain the solid product, **R-Bu-rGO-2**: ***i*-octyl-Bu-rGO-2**, **carboxymethyl-Bu-rGO-2**.

2.5. Measurement and Characterization

Transmission electron microscopy (TEM, FEI, TECNAI-20), atomic force microscope (AFM, Nanoscope IV, Digital Instruments, Veeco) were used to characterize the size and morphology of the samples. Fourier transform infrared spectroscopy (FT-IR) spectra were obtained using a Bruker Tensor 27 spectrometer. All IR samples were prepared as pellets using spectroscopic grade KBr. UV vis NIR spectra were obtained with a Jasco V-570 spectrometer. Thermal gravimetric analysis (TGA) used Netzsch STA 409PC with heating rate of 5 °C min^{-1} from room temperature to 900 °C under N_2. The conductivity of the graphene-films was measured with a Keithley 2612. Electrical conductivity characterization: As deposited films cast from graphene derivatives dispersed in ODCB or NMP by 0.5 hour sonication. After centrifugation, we obtained homogeneously dispersed solutions. Then we made the film by drop-feed method on the quartz squares substrates. After all the films are dried in vacuum at 50 °C, an Au electrode (ca. 70 nm) was deposited onto the film by thermal evaporation. The resistivity measurements were done with an electrical-probe station with a Keithley 2612.

3. RESULTS AND DISCUSSION

GO was prepared according to a modified hummers method.[40,41] We prepared rGO by reducing GO for 12 h at 100 °C in 55% hydroiodic (HI) acid under Ar.[39] As shown in Figure 2, almost all oxygen-containing groups were removed and small amount of residual carbonyl and

Delivered by Publishing Technology to: S. Rajaratnam School of International Studies, NTU
IP: 155.69.4.4 On: Wed, 25 Mar 2015 07:07:32
Copyright: American Scientific Publishers

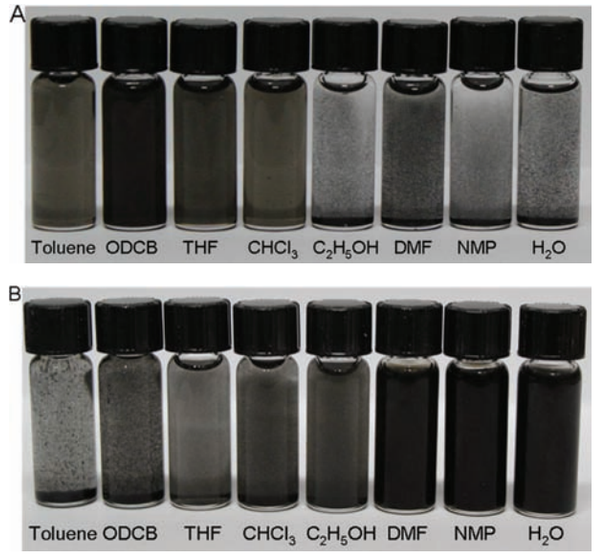

Figure 2. (A) Photograph of *i*-octyl-Bu-rGO-1 dispersing in different solvents ([*i*-octyl-Bu-rGO-1] = 0.4 mg/mL), (B) Photograph of carboxymethyl-Bu-rGO-1 dispersing in different solvents ([carboxymethyl-Bu-rGO-1] = 0.4 mg/mL), (C) Photograph of rGO dispersing in different solvents (rGO = 0.1 mg/mL).

carboxylic acid groups were distributed on the edge of graphene sheets. (see Fig. 2(C)) reactive double C═C bonds and these remaining oxygen-containing groups on the rGO sheets could react with *n*-BuLi. After reaction of *n*-BuLi with rGO sheets, $(Bu\text{-}rGO)^{n-}$ Li^{n+} was formed, which offer rich nucleophilic centers to react electrophilic reagents such as alkyl bromides to undergo nucleophilic replacement or addition with $(Bu\text{-}rGO)^{n-}$ Li^{n+} to generate functionalized graphene materials, R-Bu-rGO-1. Because excess of *n*-BuLi was added, the residual water between rGO sheets could hardly affect the reaction.

And *i*-octyl bromide and carboxymethyl bromide were chosen as coupling reagent. At last, we obtained the functionalized graphene materials *i*-octyl-Bu-rGO-1 and carboxymethyl-Bu-rGO-1, which tend to disperse in nonpolar and polar solvent, respectively.

To further check the effect of this functionalization and the controllability of the solubility, the solubility of graphene materials is tested in a series of solvents, which include toluene, ODCB, THF, CCl_3H, DMF, NMP, ethanol and water, as shown in Figure 2 and Table I. Comparing with rGO hardly dispersing in any common solvents (see Fig. 2(C)), the dispersibility in nonpolar and polar solvents of functionalized rGO was controlled by adding different alkyl bromide. When *i*-octyl bromide was used, functionalized rGO could hardly disperse in polar solvents such as NMP, water and the dispersibility in nonpolar solvents such as toluene, ODCB, increases significantly because of the presence of alkyl chains groups attaching to the functionalized GO sheets. As shown in Figure 2(A), *i*-octyl-Bu-rGO-1 is well dispersed in toluene, ODCB, THF and

Table I. Hansen solubility parameters of selected solvents. ODCB: 1,2-dichlorobenzene; CCl_3H: Chloroform; THF: tetrahydrofuran; DMF: *N*,*N*-dimethylformamide; NMP: *N*-methylpyrrolidone, δ_D: dispersion cohesion parameter, δ_P: polarity cohesion parameter, δ_H: hydrogen bonding cohesion parameter. 1: *i*-octyl-Bu-rGO-1; 2: carboxymethyl-Bu-rGO-1.

No.	Solvent	Hansen solubility parameters [$MPa^{1/2}$] δ_D	δ_P	δ_H	δ_{P+H}	Solubility of 1 mg/mL	Solubility of 2 mg/mL
1	Hexane	14.9	0.0	0.0	0.0	0.05	0.01
2	Toluene	18.0	1.4	2.0	3.4	0.16	0.01
3	ODCB	19.2	6.3	3.3	9.6	0.18	0.07
4	CCl_3H	17.8	3.1	5.7	8.8	0.09	0.02
5	THF	16.8	5.7	8.0	13.7	0.08	0.03
6	Acetone	15.5	10.4	7.0	17.4	0.06	0.17
7	DMF	17.4	13.7	11.3	25.0	0.08	0.20
8	NMP	18.0	12.3	7.2	19.5	0.02	0.58
9	C_2H_5OH	15.8	8.8	19.4	28.2	0.04	0.32
10	CH_3OH	15.1	12.3	22.3	34.6	0.04	0.20
11	H_2O	15.5	16.0	42.3	58.3	0.04	0.25

$CHCl_3$ but could not disperse in nonpolar solvents such as DMF, NMP, C_2H_5OH and water. When carboxymethyl bromide was used, because of the effect of the polar group, carboxymethyl, the dispersibility of the functionalized rGO exhibited opposite results, tending to disperse in polar solvents such as NMP, ethanol, water. As shown in Figure 2(B), carboxymethyl-Bu-GO-1 is well dispersed in DMF, NMP and water; but could not disperse in nonpolar solvents such as toluene and ODCB.

It is of importance to further evaluate the solubility of graphene materials according to Hansen Solubility Parameters (HSP), applied widely for predicting the solubility of fullerenes, carbon nanotube and grapheme.[42–45] The functionalized graphene materials: *i*-octyl-Bu-rGO-1 dispersed in toluene, ODCB, THF, CCl_3H with the value of δ_{P+H} in the range of 3–14, while carboxymethyl-Bu-rGO-1 dispersed in aceton, DMF, NMP, ethanol, methanol and water with the value of δ_{P+H} in the range of 17–59. (see Table I) These results fully prove that this functional method is effective for improving the dispersibility of graphene materials in solvent and more significantly, we can control the dispersibility in nonpolar and polar solvents of graphene materials by adding different alkyl bromide in the functionalized reaction.

Further characterizing the functionalized graphene materials by FTIR (see Fig. 3), TGA (see Fig. 4), TEM (see Fig. 5) and AFM (see Fig. 6) confirmed the successful functionalization.

As shown in Figure 3, the intense absorption peaks at 2957 cm^{-1}, 2925 cm^{-1}, 2854 cm^{-1} are attributed to the stretching vibration of $-CH_2-$ and $-CH_3$. The peaks at 1447 cm^{-1}, 1385 cm^{-1} are attributed to the deformation vibration of $-CH_2-$. Furthermore, the new absorption peak at 1575 cm^{-1} in *i*-octyl-Bu-rGO-1 indicated that the C═H

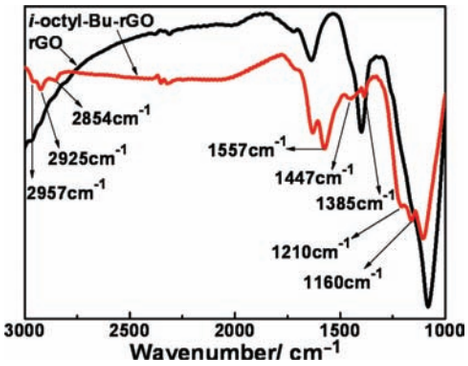

Figure 3. FTIR spectra of rGO, *i*-octyl-Bu-rGO-1. Strong stretching vibration of C–H at 2957 cm^{-1}, 2925 cm^{-1}, 2854 cm^{-1} in *i*-octyl-Bu-rGO-1 indicates functional alkyl chain groups are chemically attached to the graphene sheets.

on aromatic ring greatly increased after functionalization. New peaks at 1210 cm^{-1} and 1160 cm^{-1} corresponding to the O-Ar and O-R (R = 2-Ethylhexyl) stretching vibration are clearly observed, which indicates the 2-Ethylhexyl bromide reacts with the $(Bu\text{-}rGO)^{n-}Li^{n+}$. These all conformed that through the generic organometallic reaction the alkyl groups were successfully attached onto the large aromatic ring.

Figure 4 shows the TGA curves of the rGO and *i*-octyl-Bu-rGO-1. Reduced GO (rGO) is thermally stable and there was no obvious weight loss below 634 °C, which indicated that after reduction by HI, the most oxygen-containing functional groups of GO were removed. After 634 °C, the obvious weight loss was attributed to the pyrolysis of graphene's framework. Compared with the curve of graphene, the weight loss of *i*-octyl-Bu-rGO-1 below 500 °C is lower. Between 500 °C and 640 °C, It shows a fast weight loss of ca. 50 %, which was attributed to the remove of functionalized alkyl chains. These results demonstrate that *i*-octyl-Bu-rGO-1 has worse thermal stability than rGO.

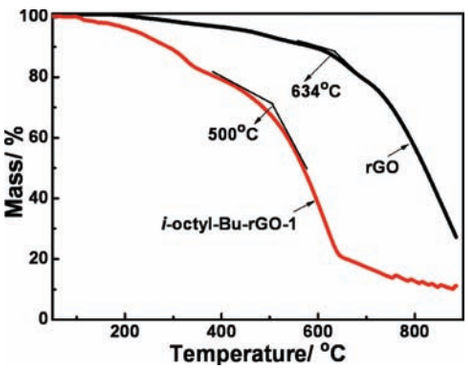

Figure 4. TGA curves of rGO and *i*-octyl-Bu-rGO-1 were obtained with a heating rate of 5 °C min^{-1} under purified nitrogen gas flow. Compared with rGO, there was an obvious weight loss of *i*-octyl-Bu-rGO-1 at 500 °C, indicating the functional groups made rGO thermal unstability.

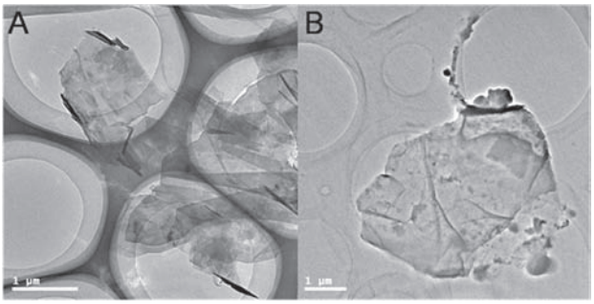

Figure 5. (A) TEM images of GO, (B) TEM images of *i*-octyl-Bu-rGO-1.

TEM measurements have also been performed. The resulting GO (in water) and *i*-octyl-Bu-rGO-1 (in ODCB) dispersions of 0.1 mg mL^{-1} were placed directly on two Cu grids and examined under a transmission electron microscope (TEM). We could not take TEM measurements of rGO, due to it was insoluble in any solvent. The materials of GO sheets which we used in the reaction were monolayer dispersed, smooth and transparent, as shown in Figure 5(A). The TEM images of *i*-octyl-Bu-rGO-1 (see Fig. 5(B)) show that mostly single layers with few layers and small flakes stacked on top. The morphology and well dispersion of *i*-octyl-Bu-rGO-1 sheets obtained in this work, which is very important for further preparation of nanocomposite materials based on graphene.

We employed AFM to establish the thickness and surface roughness of the depositions. The samples were prepared by depositing well-dispersed *i*-octyl-Bu-rGO-1 in ODCB (0.1 mg mL^{-1}) on new cleaved mica surfaces and drying in air. AFM images of *i*-octyl-Bu-rGO-1 in Figure 6 show the areas in which single sheets with a thickness of about 0.8 nm are present, and with different lateral dimensions between 20 and 200 nm. Compared

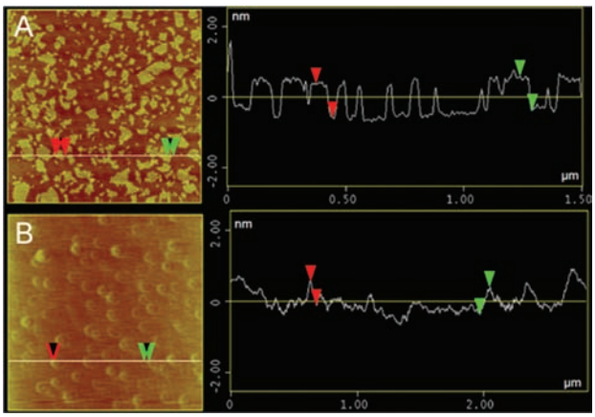

Figure 6. (A) AFM image of GO sheets on a mica surface. (B) AFM image of *i*-octyl-Bu-rGO-1 sheets on a mica surface. Single sheets of *i*-octyl-Bu-rGO-1 with an average thickness of about 0.8 nm are present, with different lateral dimensions between 20 and 200 nm.

with images of GO shown in Figure 5(A), no matter functionalization or reduction, the size and thickness of graphene sheets have no obvious change, which is consistent with a single layer of functionalized GO and graphene. Although many alkyl chains attached to the surface or edge but were relatively short and flexible, it has little effect on the thickness of graphene sheets.

As shown in the results above, the organometallic approach was feasible for functionalization of rGO. However, the functional groups on the graphene sheets are disadvantage to many applications, so removal of the functional groups on the graphene sheet is sometimes needed. In that case, it is required that the functionalized methods must be reversible. To investigate the reversibility of this functionalized method we used, the functionalized graphene materials, *i*-octyl-Bu-rGO-1 and carboxymethyl-Bu-rGO-1 would be solvothermally reduced and functionalized once more using the same sequence reactions, as shown in Figure 7. And the reversibility of this functionalized method was in detail investigated by elemental analysis, TGA, Raman spectroscopy and electrical conductivity.

Figure 7 showed the scheme for the solvothermal reduction functionalized rGO and the second functionalization using the same method as shown in Figure 1. The method of reduction of GO by solvothermal reduction have been widely studied,[46,47] which was conformed as a simple, green and effective way to obtain dispersible graphene. The solvothermal reduction method we used utilizes the high boiling point of ODCB and NMP to remove the functional groups.[47,48] We carried the solvothermal reduction of *i*-octyl-Bu-rGO-1 in refluxed ODCB under Ar flow for their good dispersibility in ODCB, to obtain the reduced products *i*-octyl-Bu-rGO-R, respectively. By same means, carboxymethyl-Bu-rGO-1 was reduced in refluxed NMP to obtain the products carboxymethyl-Bu-rGO-R. In the solvothermal reduction, the removed alkyl groups connected to the graphene carbon by C—C could be back by the second functionalization. In the solvothermal reduction, part of products precipitated from solvent which

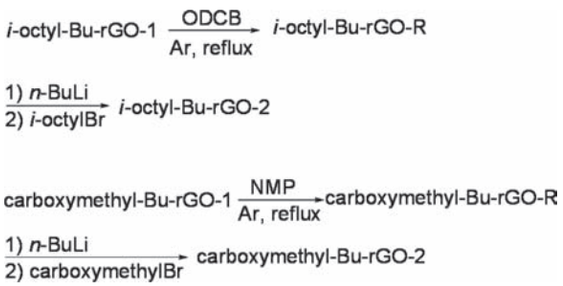

Figure 7. The scheme for solvothermal reduction reaction of the functionalized materials to obtain reduced materials: *i*-octyl-Bu-rGO-R, carboxymethyl-Bu-rGO-R and the second functionalization to obtain *i*-octyl-Bu-rGO-2, carboxymethyl-Bu-rGO-2 using the same method as above.

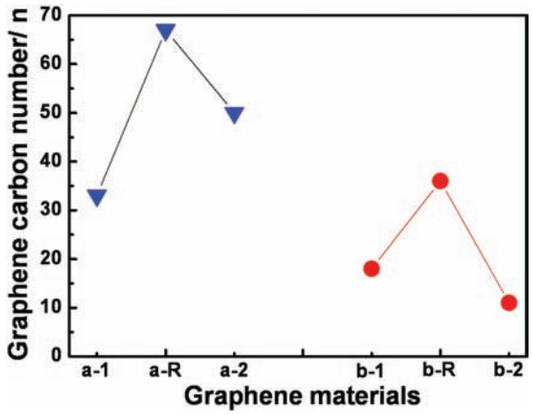

Figure 8. Graphene carbon number (n) was calculated to be one functional group per n graphene carbons. It was estimated according to the mass ratio from elemental analysis of rGO and functionalized rGO, (a-1, a-R, a-2) *i*-octyl-Bu-rGO-1, *i*-octyl-Bu-rGO-R and *i*-octyl-Bu-rGO-2; (b-1, b-R, b-2) carboxymethyl-Bu-rGO-1, carboxymethyl-Bu-rGO-R and carboxymethyl-Bu-rGO-2.

illustrated the dispersion of the reduced products in solvent worsened. But until the end of reduced reaction, most of the reduced products could still disperse in reaction solvents.

As Figure 8 shown, graphene carbon number (n) was calculated to be one functional group per n graphene carbons. It was estimated according to the mass ratio from elemental analysis of functionalized rGO. (see Table II) The degree of functionalization for *i*-octyl-Bu-rGO-1 was estimated to be one functional group per ~30 graphene carbons, with carboxymethyl-Bu-rGO-1 ~20 graphene carbons. After solvothermal reduction, the degree of functionalization for *i*-octyl-Bu-rGO-R was estimated to be one functional group per ~60 graphene carbons, with carboxymethyl-Bu-rGO-R ~36 graphene carbons. About half of functional groups were removed after the solvothermal reduction. Then the elemental analysis of *i*-octyl-Bu-rGO-2 and carboxymethyl-Bu-rGO-2 showed that about equivalent groups with that removed by reduction were covalently attached to rGO sheets through the second functionalization. These indicated that reductive retrofunctionalization of rGO was reversible.

Table II. Elemental analysis of rGO and functionalized rGO. And according to the mass ratio, n was calculated to estimate the degree of functionalization. (a) The degree of functionalization on rGO was estimated to be one functional group per n carbons.

Samples	C/%	H/%	n[a]
rGO	62.15	1.56	
i-octyl-Bu-rGO-1	66.19	3.15	33
i-octyl-Bu-rGO-R	50.25	2.43	67
i-octyl-Bu-rGO-2	58.76	3.15	50
Carboxymethyl-Bu-rGO-1	58.93	3.55	18
Carboxymethyl-Bu-rGO-R	53.51	2.44	36
Carboxymethyl-Bu-rGO-2	64.14	5.04	11

Delivered by Publishing Technology to: S. Rajaratnam School of International Studies NTU
Date: Wed, 25 Mar 2015 07:07:22
Copyright: American Scientific Publishers

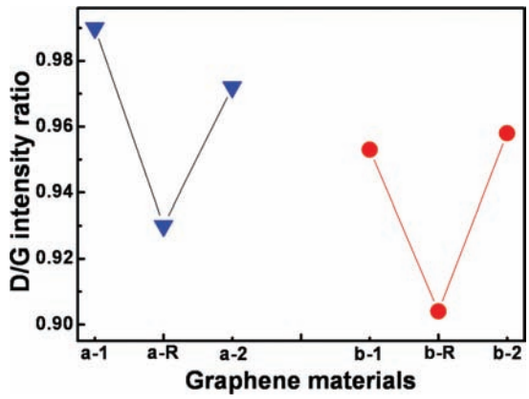

Figure 9. Raman spectra of (a-1, a-R, a-2) *i*-octyl-Bu-rGO-1, *i*-octyl-Bu-rGO-R and *i*-octyl-Bu-rGO-2; (b-1, b-R, b-2) carboxymethyl-Bu-rGO-1, carboxymethyl-Bu-rGO-R and carboxymethyl-Bu-rGO-2.

The variation of the relative intensities of G (the E2g mode of sp^2 carbon atoms) and D (the symmetry A1g mode) bands in the Raman spectra of the graphene materials during the reduction usually reveals the change of the electronic conjugation state. Among the process of reduction and second-functionalization, there was no remarkable change of the position of the peaks. (see Fig. 10) While the ratio of the intensities (ID/IG) for *i*-octyl-Bu-rGO-1, *i*-octyl-Bu-rGO-R, *i*-octyl-Bu-rGO-2, 0.990, 0.930, 0.972; for carboxymethyl-Bu-rGO-1, carboxymethyl-Bu-rGO-R, carboxymethyl-Bu-rGO-2, 0.953, 0.904, 0.958. As depicted in Figure 9, while the ratio of the intensities (ID/IG) for the four group data showed the same change regulation: after solvothermal reduction, the ratio of the intensities (I_D/I_G) of the samples decreased, which indicated that some sp^3-carbon was converted to sp^2-carbon on the graphene sheets and after the functionalization of reduced-materials, the ratio of the intensities (I_D/I_G) of the samples creased to almost the same as samples of before-reduction which indicated that almost the same amount sp^2-carbon was converted to sp^3-carbon. The small change of the relative intensities (I_D/I_G) before and after the reduction was thought that the elemental analysis show only half functional groups were removed and the large π-conjugation structure of graphene was only partly restored. Even so, the extent and tendency of the change demonstrate that this method of reductive retrofunctionalization for the graphene materials was reversible.

Delivered by Publishing Technology to: S. Rajaratnam School of International Studies, NTU
IP: 155.69.4.4 On: Wed, 25 Mar 2015 07:07:32
Copyright: American Scientific Publishers

Table III. Comparison of the dependence of sheet resistance and film (100–300 nm thickness) and conductivity of *i*-octyl-Bu-rGO-1, *i*-octyl-Bu-rGO-R, *i*-octyl-Bu-rGO-2; carboxymethyl-Bu-rGO-1, carboxymethyl-Bu-rGO-R, carboxymethyl-Bu-rGO-2.

Graphene Films	Sheet Resistance (Ω/sq)	Film Conductivity (S/cm)
i-octyl-Bu-rGO-1	$1.40 * 10^8$	$4.78 * 10^{-4}$
i-octyl-Bu-rGO-R	$2.05 * 10^6$	$1.86 * 10^{-2}$
i-octyl-Bu-rGO-2	$2.25 * 10^8$	$1.39 * 10^{-4}$
Carboxymethyl-Bu-rGO-1	$5.20 * 10^8$	$8.49 * 10^{-5}$
Carboxymethyl-Bu-rGO-R	$6.21 * 10^6$	$4.54 * 10^{-3}$
Carboxymethyl-Bu-rGO-2	$2.24 * 10^8$	$2.04 * 10^{-4}$

Generally, electrical conductivity of graphene materials could reflect well both the extent of the reduction and the restoration of the electronic conjugation state.[49] So, room-temperature electrical conductivities of the samples of functionalized graphene materials at every stage were measured. (see Table III) At a given film thickness of ca. 100–300 nm, concomitant increase of film conductivity was observed with about an one or two degree increase after solvothermal reduction which is attributed the content of graphite structure recovered; (see Fig. 11) and after the functionalization of the reduced-materials, film conductivity of the samples reduced to almost the same as samples of before-reduction which indicated that almost the same amount sp^3-carbon was converted to sp^2-carbon in the solvothermal reduction as that sp^2-carbon was converted to sp^3-carbon in the functionalization. All these could demonstrate that this method of reductive retrofunctionalization for the graphene materials was reversible.

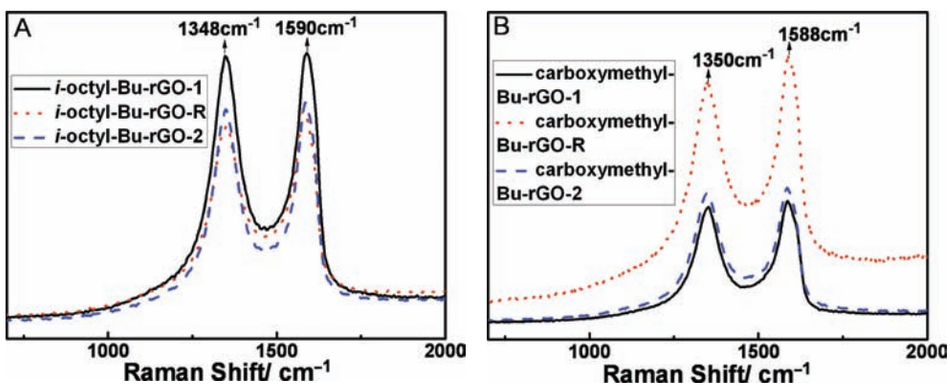

Figure 10. Raman spectra of (A) *i*-octyl-Bu-rGO-1, *i*-octyl-Bu-rGO-R, i-octyl-Bu-rGO-2; (B) carboxymethyl-Bu-rGO-1, carboxymethyl-Bu-rGO-R, carboxymethyl-Bu-rGO-2.

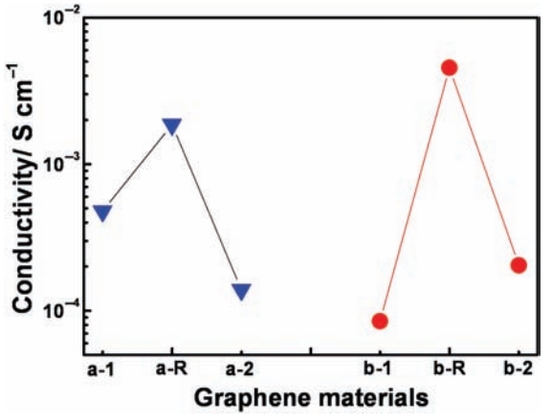

Figure 11. Conductivity of graphene materials: (a-1, a-R, a-2) *i*-octyl-Bu-rGO-1, *i*-octyl-Bu-rGO-R and *i*-octyl-Bu-rGO-2; (b-1, b-R, b-2) carboxymethyl-Bu-rGO-1, carboxymethyl-Bu-rGO-R and carboxymethyl-Bu-rGO-2.

4. CONCLUSIONS

In conclusion, we have showed that the generic organometallic approach to functionalize rGO was an effective way to obtain solution-processable graphene materials in common organic solvents. The dispersibility in nonpolar and polar solvents of graphene materials can be controlled by adding different alkyl bromide in the coupling reaction. And the nucleophilic additions to the plane of rGO are reversible. As a consequence retro-functionalization of graphene derivatives can be achieved under mild conditions simply by solvothermal reduction. The variation of elemental analysis, Raman spectroscopy and film conductivity gave the strong evidence that the functional groups of the samples could be half removed by solvothermal reduction. The reduced samples could be again functionalized to almost the same functionalization degree using the same method above. We thought these methods would bring important significance to the application of graphene-based materials and device.

Delivered by Publishing Technology to: S. Rajaratnam School of International Studies, NTU
IP: 155.69.4.4 On: Wed, 25 Mar 2015 07:07:32
Copyright: American Scientific Publishers

Acknowledgments: The authors gratefully acknowledge the financial support from the NSFC (#50933003, 50903044), MOST (#2009AA032304 [863], 2011CB932602) and NSF of Tianjin City (#08JCZDJC25300) of China.

References and Notes

1. K. S. Novoselov, A. K. Geim, S. V. Morozov, D. Jiang, Y. Zhang, S. V. Dubonos, I. V. Grigorieva, and A. A. Firsov, *Science* 306, 666 (**2004**).
2. Y. B. Zhang, J. W. Tan, H. L. Stormer, and P. Kim, *Nature* 438, 201 (**2005**).
3. A. K. Geim and K. S. Novoselov, *Nat. Mater.* 6, 183 (**2007**).
4. X. L. Li, X. R. Wang, L. Zhang, S. Lee, and H. J. Dai, *Science* 319, 1229 (**2008**).
5. S. Stankovich, D. A. Dikin, G. H. B. Dommett, K. M. Kohlhaas, E. J. Zimney, E. A. Stach, R. D. Piner, S. T. Nguyen, and R. S. Ruoff, *Nature* 442, 282 (**2006**).
6. S. Watcharotone, D. A. Dikin, S. Stankovich, R. Piner, I. Jung, G. H. B. Dommett, G. Evmenenko, S. E. Wu, S. F. Chen, C. P. Liu, S. T. Nguyen, and R. S. Ruoff, *Nano Lett.* 7, 1888 (**2007**).
7. X. Huang, X. Y. Qi, F. Boey, and H. Zhang, *Chem. Soc. Rev.* 41, 666 (**2012**).
8. X. Huang, Z. Y. Yin, S. X. Wu, X. Y. Qi, Q. Y. He, Q. C. Zhang, Q. Y. Yan, F. Boey, and H. Zhang, *Small* 7, 1876 (**2011**).
9. X. Huang, S. Z. Li, Y. Z. Huang, S. X. Wu, X. Z. Zhou, S. Z. Li, C. L. Gan, F. Boey, C. A. Mirkin, and H. Zhang, *Nat. Commun.* 2, 292 (**2011**).
10. X. Y. Qi, K.-Y. Pu, H. Li, X. Z. Zhou, S. X. Wu, Q.-L. Fan, B. Liu, F. Boey, W. Huang, and H. Zhang, *Angew. Chem. Int. Ed.* 49, 9426 (**2010**).
11. X. Y. Qi, K.-Y. Pu, X. Z. Zhou, H. Li, B. Liu, F. Boey, W. Huang, and H. Zhang, *Small* 6, 663 (**2010**).
12. X. H. Cao, Q. Y. He, W. H. Shi, B. Li, Z. Y. Zeng, Y. M. Shi, Q. Y. Yan, and H. Zhang, *Small* 7, 1199 (**2011**).
13. X. Huang, H. Li, S. Z. Li, S. X. Wu, F. Boey, J. Ma, and H. Zhang, *Angew. Chem. Int. Ed.* 50, 12245 (**2011**).
14. Z. F. Liu, Q. Liu, X. Y. Zhang, Y. Huang, Y. F. Ma, S. G. Yin, and Y. S. Chen, *Adv. Mater.* 20, 3924 (**2008**).
15. C. E. Hamilton, J. R. Lomeda, Z. Z. Sun, J. M. Tour, and A. R. Barron, *Nano Lett.* 9, 3460 (**2009**).
16. S. Gilje, S. Han, M. S. Wang, K. L. Wang, and R. B. Kaner, *Nano Lett.* 7, 3394 (**2007**).
17. X. Wang, L. J. Zhi, and K. Müllen, *Nano Lett.* 8, 323 (**2008**).
18. D. Li, M. B. Müller, S. Gilje, R. B. Kaner, and G. G. Wallace, *Nat. Nanotechnol.* 3, 101 (**2008**).
19. D. R. Dreyer, S. Park, C. W. Bielawski, and R. S. Ruoff, *Chem. Soc. Rev.* 39, 228 (**2010**).
20. J. C. Hummelen, B. W. Knight, F. LePeq, and F. Wudl, *J. Org. Chem.* 60, 532 (**1995**).
21. V. Georgakilas, K. Kordatos, M. Prato, D. M. Guldi, M. Holzinger, and A. Hirsch, *J. Am. Chem. Soc.* 124, 760 (**2002**).
22. Y. Zhu and J. M. Tour, *Nano Lett.* 10, 4356 (**2010**).
23. Y. F. Xu, Z. B. Liu, X. L. Zhang, Y. Wang, J. G. Tian, Y. Huang, Y. F. Ma, X. Y. Zhang, and Y. S. Chen, *Adv. Mater.* 21, 1275 (**2009**).
24. K. P. Loh, Q. Bao, P. K. Ang, and J. Yang, *J. Mater. Chem.* 20, 2277 (**2010**).
25. S. H. Cheng, K. Zou, F. Okino, H. R. Gutierrez, A. Gupta, N. Shen, P. C. Eklund, and J. O. Sofo, *Phys. Rev. B* 81, 205435 (**2010**).
26. E. Bekyarova, M. E. Itkis, P. Ramesh, C. Berger, M. Sprinkle, W. A. de Heer, and R. C. Haddon, *J. Am. Chem. Soc.* 131, 1336 (**2009**).
27. X. Huang, Z. Y. Zeng, Z. X. Fan, J. Q. Liu, and H. Zhang, *Adv. Mater.* 24, 5979 (**2012**).
28. Q. Y. He, S. X. Wu, Z. Y. Yin, and H. Zhang, *Chem. Sci.* 3, 1764 (**2012**).
29. Q. Y. He, S. X. Wu, S. Gao, X. H. Cao, Z. Y. Yin, H. Li, P. Chen, and H. Zhang, *ACS Nano* 5, 5038 (**2011**).
30. Z. Y. Yin, S. Y. Sun, T. Salim, S. X. Wu, X. Huang, Q. Y. He, Y. M. Lam, and H. Zhang, *ACS Nano* 4, 5263 (**2010**).
31. G. Viswanathan, N. Chakrapani, H. Yang, B. Q. Wei, H. Chung, K. Cho, C. Y. Ryu, and P. M. Ajayan, *J. Am. Chem. Soc.* 125, 9258 (**2003**).
32. R. Graupner, J. Abraham, D. Wunderlich, A. Vencelová, P. Lauffer, J. Röhrl, M. Hundhausen, L. Ley, and A. Hirsch, *J. Am. Chem. Soc.* 128, 6683 (**2006**).
33. A. Hirsch, A. Soi, and H. R. Karfunhel, *Angew. Chem. Int. Ed. Engl.* 31, 766 (**1992**).
34. K. A. Worsley, P. Ramesh, S. K. Mandal, S. Niyogi, M. E. Itkis, and R. C. Haddon, *Chem. Phys. Lett.* 445, 51 (**2007**).
35. Y. J. Huang, Y. W. Qin, Y. Zhou, H. Niu, Z. Z. Yu, and J. Y. Dong, *Chem. Mater.* 22, 4096 (**2010**).
36. S. Park and R. S. Ruoff, *Nat. Nanotechnol.* 4, 217 (**2009**).
37. H. Gilman, F. W. Moore, and O. Baine, *Interconversion Reactions with Alkyllithium Compounds* 63, 2479 (**1941**).

38. Y. Maeda, T. Kato, T. Hasegawa, M. Kako, T. Akasaka, J. Lu, and S. Nagase, *Org. Lett.* 12, 996 **(2010)**.
39. S. Pei, J. Zhao, J. Du, W. Ren, and H. Cheng, *Carbon* 48, 4466 **(2010)**.
40. W. S. Hummers, Jr and R. E. Offeman, *J. Am. Chem. Soc.* 80, 1339 **(1958)**.
41. H. A. Becerril, J. Mao, Z. F. Liu, R. M. Stoltenberg, Z. N. Bao, and Y. S. Chen, *ACS Nano* 2, 463 **(2008)**.
42. K. N. Kudin, B. Ozbas, H. C. Schniepp, R. K. Prud'homme, I. A. Aksay, and R. Car, *Nano Lett.* 8, 36 **(2008)**.
43. R. S. Ruoff, D. S. Tse, R. Malhotra, and D. C. Lorents, *J. Phys. Chem.* 97, 3379 **(1993)**.
44. K. D. Ausman, R. Piner, O. Lourie, and R. S. Ruoff, *J. Phys. Chem. B* 104, 8911 **(2000)**.
45. S. Park, J. An, I. Jung, R. D. Piner, S. J. An, X. Li, A. Velamakanni, and R. S. Ruoff, *Nano Lett.* 9, 1593 **(2009)**.
46. Y. Zhou, Q. Bao, L. Tang, Y. Zhong, and K. Loh, *Chem. Mater.* 21, 2950 **(2009)**.
47. S. Dubin, S. Gilje, K. Wang, V. C. Tung, K. Cha, A. S. Hall, J. Farrar, R.Varshneya, Y. Yang, and R. B. Kaner, *Acs. Nano* 4, 3845 **(2010)**.
48. H. L. Wang, J. T. Robinson, X. L. Li, and H. J. Dai, *J. Am. Chem. Soc.* 131, 9910 **(2009)**.
49. V. C. Tung, M. J. Allen, Y. Yang, and R. B. Kaner, *Nat. Nanotechnol.* 4, 25 **(2009)**.

Received: 10 June 2013. Accepted: 30 October 2013.

Delivered by Publishing Technology to: S. Rajaratnam School of International Studies, NTU
IP: 155.69.4.4 On: Wed, 25 Mar 2015 07:07:32
Copyright: American Scientific Publishers